Stockholder projector analysis: A Hilbert-space partitioning of the molecular one-electron density matrix with orthogonal projectors

Diederik Vanfleteren, Dimitri Van Neck, Patrick Bultinck, Paul W. Ayers, and Michel Waroquier

Citation: J. Chem. Phys. **136**, 014107 (2012); doi: 10.1063/1.3673321
View online: http://dx.doi.org/10.1063/1.3673321
View Table of Contents: http://jcp.aip.org/resource/1/JCPSA6/v136/i1
Published by the American Institute of Physics.

Stockholder projector analysis: A Hilbert-space partitioning of the molecular one-electron density matrix with orthogonal projectors

Diederik Vanfleteren,[1,2,a)] Dimitri Van Neck,[1,2] Patrick Bultinck,[1,3] Paul W. Ayers,[4] and Michel Waroquier[1,2]

[1]*Members of the Ghent Brussels Quantum Chemistry and Molecular Modelling alliance*
[2]*Ghent University, Center for Molecular Modeling, Technologiepark 903, B-9052 Zwijnaarde, Belgium*
[3]*Ghent University, Department of Inorganic and Physical Chemistry, Krijgslaan 281 (S3), B-9000 Gent, Belgium*
[4]*McMaster University, Department of Chemistry, Hamilton, Ontario L8S 4M1, Canada*

(Received 27 July 2011; accepted 8 December 2011; published online 4 January 2012)

A previously introduced partitioning of the molecular one-electron density matrix over atoms and bonds [D. Vanfleteren *et al.*, J. Chem. Phys. **133**, 231103 (2010)] is investigated in detail. Orthogonal projection operators are used to define atomic subspaces, as in Natural Population Analysis. The orthogonal projection operators are constructed with a recursive scheme. These operators are chemically relevant and obey a stockholder principle, familiar from the Hirshfeld-I partitioning of the electron density. The stockholder principle is extended to density matrices, where the orthogonal projectors are considered to be atomic fractions of the summed contributions. All calculations are performed as matrix manipulations in one-electron Hilbert space. Mathematical proofs and numerical evidence concerning this recursive scheme are provided in the present paper. The advantages associated with the use of these stockholder projection operators are examined with respect to covalent bond orders, bond polarization, and transferability. © *2012 American Institute of Physics*. [doi:10.1063/1.3673321]

I. INTRODUCTION

Many successful theories in chemistry are based on the concept of atoms (and bonds) in molecules (AIM). Numerous attempts were made to get a quantum mechanical description of these AIM subsystems. Early techniques focussed on determining electron densities for atoms in molecules. This can be done in Hilbert space (the Mulliken population analysis[1]) or in 3D space, using either nonoverlapping atomic basins (e.g., Bader's quantum theory of atoms in molecules[2–4]) or overlapping atomic regions (e.g., the standard Hirshfeld method[5]). In Bader's quantum theory of atoms in molecules (QTAIM), a "zero-flux" boundary condition for the electron density is satisfied at every point of an interatomic surface. The interatomic surface delimits the atomic domains. This implies that $\boldsymbol{r}$-space is partitioned in a binary way, since each point in space corresponds completely to a single atomic domain Ω_A. In the standard Hirshfeld method, a model electron density for the molecule $\rho^0(\boldsymbol{r})$ is constructed from the electron densities $\rho_A^0(\boldsymbol{r})$ of neutral isolated atoms placed at the positions of the nuclei in the molecule, and the overlapping atomic regions are defined by the contribution of each isolated atom to the model electron density. Perceived deficiencies in the standard Hirshfeld method (a dependence on the charge and state of the isolated atoms) are addressed in the Hirshfeld-I technique (the iterative version of the Hirshfeld method[6–9]) and the iterative stockholder approach (ISA)[10]).

Although these methods are well-established techniques that are widely used, ambiguities arise with respect to calculating the properties of the resulting atomic densities. A way to overcome these difficulties for one-electron operators, is to determine the full atom-condensed one-electron density matrices (1DM). The expectation values for one-electron operators are naturally (and unambiguously) expressed in terms of the one-electron density matrices (1DMs).[11] We recently proposed atom-condensed 1DMs for the Hirshfeld-I AIM model[12] and determined the energy components of the Hirshfeld-I fragments.[13] These atom-condensed 1DMs are actually based on a partitioning of the molecular density matrix over atoms and bonds in molecules (ABIM). Because molecular 1DMs are inherently nonlocal, a two-index partitioning into atomic (diagonal) and bond (off-diagonal) contributions is necessary to guarantee the local nature and transferability of the atoms.[12,14] However, we observed that these bond fragments have a rather complicated structure, as large positive and smaller negative eigenvalues appear in the bond matrix. A much simpler bond structure can be obtained when orthogonal projectors are used to define atomic and bond regions in the molecule.[15]

We therefore tried to optimize the ABIM description. In a recently introduced scheme[15] for defining the atomic and bond fragments of the molecular 1DM, we combined the recipes of the different existing techniques. (i) All calculations are performed as matrix manipulations in one-electron Hilbert space, making it highly efficient in terms of computation time, since no grid-based numerical integrations are needed. (ii) For interpretative convenience, orthogonal projection operators are used to define atomic subspaces of one-electron Hilbert space. Note that the concept of using orthogonal projectors has a

a)Author to whom correspondence should be addressed. Electronic mail: diederik_vanfleteren@yahoo.co.uk.

long history dating back to Löwdin's work on population analysis.[16–20] Perceived deficiencies of Löwdin's populations are addressed in Natural Population Analysis (NPA),[21] a well-known technique based on orthogonalizing atomic subblocks of the molecular density matrix. (iii) In contrast to NPA-based schemes, the orthogonal projection operators are determined iteratively by a stockholder approach starting from 1DMs of the isolated atoms. Stockholder techniques, as used in the standard Hirshfeld and the ISA approach to atomic partitioning of the electron density, are known to minimize the information loss in the Kullback-Leibler information entropy sense,[22–24] and therefore maximally preserve the structure of the reference atoms. In the present case we find that chemical relevance and transferability of the resulting atoms and bonds seem to follow quite naturally in such a stockholder approach. (iv) The projection operators can then be used to define density matrices assigned to atoms and bonds in the molecule. Reminiscent of the Hirshfeld-I approach, an outer iterative procedure ensures that the reference atoms (that are needed to initiate the stockholder procedure) are optimally chosen.

The new scheme will be referred to as stockholder projector analysis (SPA). Preliminary results obtained with this scheme were promising:[15] the bond fragments of the 1DM can be soundly interpreted in terms of a transfer of electrons from antibonding to bonding orbitals, and have no contributions from core electrons and free electron pairs. The atomic fragments of the 1DM are well localized and the atomic charges correlate linearly with well-established Hirshfeld-I charges. Atomic populations and bond occupancies converge efficiently with respect to basis set size.

The present paper is a continuation of this preliminary work.[15] In Secs. II and III, the theoretical background of the method is analyzed. We provide proof for the assumption that chemically relevant orthogonal projection operators can be constructed using a recursive scheme. In Sec. IV, we examine the advantages associated with the use of orthogonal projection operators from a stockholder approach. In Sec. V, similarities and differences between the new SPA approach and the NPA technique are discussed. In Sec. VI, we provide numerical results for the SPA approach with respect to transferability, bond orders and bond polarization for a representative subset of ca. 70 small molecules.

II. ORTHOGONAL PROJECTORS FROM A STOCKHOLDER APPROACH: RECURSIVE SCHEMES AND PROOFS

In a previous paper,[15] we introduced a double-atom partitioning scheme for the molecular spin-summed one-electron density matrix,

$$\rho = \sum_{AB} \rho_{AB}, \tag{1}$$

in terms of atomic (AA) and bond ($A \neq B$) contributions. All calculations are performed in the one-electron Hilbert space, i.e., all ρ_{AB} are matrices with elements $(\rho_{AB})_{ij}$ where indices i, j refer to an orthogonal basis set. The individual contributions are defined as

$$\rho_{AB} = \frac{1}{2}\left(w_A \rho w_B + w_B \rho w_A\right) \tag{2}$$

in which the concept of atomic weight functions (familiar from Hirshfeld analysis of the electron density) is extended to atomic weight matrices w_A obeying

$$\delta_{ij} = \sum_A (w_A)_{ij}. \tag{3}$$

The atomic weight matrices are constructed as orthogonal projection operators on one-electron atomic subspaces, i.e., they fulfill the following relation:

$$w_A w_B = w_A \delta_{AB}. \tag{4}$$

As a consequence, the ρ_{AA} can be regarded as 1DMs of atoms that are excited by the molecular environment but still contain the full number of electrons N,

$$N = Tr(\rho) = \sum_A Tr(\rho_{AA}). \tag{5}$$

No electrons are lost to the bonds ($Tr(\rho_{AB}) = 0$ for $A \neq B$), which is a significant advantage in the interpretation of the atomic and bond contributions. This is a marked difference with the ABIM approach in a previous paper,[12] where we reported significant bond traces. Starting from the 1DMs $\rho_{AA}^{(0)}$ of isolated atoms, the following recursive scheme ($i = 0, 1, \ldots$):

$$\rho^{(i)} = \sum_A \rho_{AA}^{(i)}; \quad w_A^{(i)} = (\rho^{(i)})^{-\frac{1}{2}} \rho_{AA}^{(i)} (\rho^{(i)})^{-\frac{1}{2}},$$
$$\rho_{AA}^{(i+1)} = w_A^{(i)} \rho w_A^{(i)}, \tag{6}$$

converges and generates weight matrices $w_A^{(\infty)}$ that both obey Eq. (4) and can be applied in Eq. (2) to produce a chemically relevant decomposition. Henceforth, the superscript $^{(\infty)}$ is used to indicate that recursive scheme has converged. Typically, the scheme reaches convergence in less than 10 iterations. Upon convergence, $\rho^{(\infty)}$ contains the summed atomic 1DMs and therefore represents the molecular 1DM stripped of its bond contributions.

The recursive scheme of Eq. (6) can be generalized and rewritten more compactly,

$$w_A^{(i)} = (\rho^{(i)})^{-\frac{1}{2}} w_A^{(i-1)} M w_A^{(i-1)} (\rho^{(i)})^{-\frac{1}{2}},$$
$$\rho^{(i)} = \sum_A w_A^{(i-1)} M w_A^{(i-1)}, \tag{7}$$

where M is in general any positive-definite matrix. To obtain a chemically meaningful decomposition, we found that M can be chosen as either the full molecular 1DM itself ($M = \rho$ as in Eq. (6)), or the recursive estimate for $\rho^{(\infty)}$ (with $M = \rho^{(i-1)}$ in Eq. (7)). The preferred choice depends on the starting point for the recursive scheme.

The recursion is applied to transform initial weight matrices to orthogonal projectors on one-electron subspaces (see Eq. (4)). It can be proven that every set of orthogonal

projectors is a solution to the convergence limit of Eq. (7),

$$w_A^{(\infty)} = (\rho^{(\infty)})^{-\frac{1}{2}} w_A^{(\infty)} M w_A^{(\infty)} (\rho^{(\infty)})^{-\frac{1}{2}},$$
$$\rho^{(\infty)} = \sum_A w_A^{(\infty)} M w_A^{(\infty)}. \quad (8)$$

If upon convergence M equals $\rho^{(\infty)}$, then these are also the only solutions to Eq. (8). If M equals ρ, then the sets of orthogonal projectors are only part of the entire solution set. This follows from the following lemmas, the proof of which is contained in the appendix:

Lemma 2.1. *If $M = \rho^{(i-1)}$ in Eq. (7), then the converged atomic weight matrices $w_A^{(\infty)}$ are idempotent.*

Lemma 2.2. *If the converged weight matrices $w_A^{(\infty)}$ are idempotent, then they are orthogonal.*

Lemma 2.3. *When idempotent weight matrices enter the recursion formula, immediate convergence is obtained.*

Lemma 2.4. *If $M = \rho$ in Eq. (7), then non-idempotent solutions to Eq. (8) exist.*

For $M = \rho$, it is in principle not excluded that particular non-idempotent solutions to Eq. (8) result from the recursion. However, in our investigation only idempotent solutions were obtained for any choice of the starting point. We included numerical evidence in the results section of the paper, demonstrating that for every molecule in the test set the recursion of Eq. (7) always transformed the initial weight matrices into perfect orthogonal projectors.

III. STARTING POINTS FOR STOCKHOLDER PROJECTORS

The choice of the starting point in the recursive scheme of Eq. (6) is crucial, as the chemical relevance of the resulting stockholder projectors is largely inherited from the starting point. The starting point is either a trial weight matrix $w_A^{(0)}$ or a trial atomic 1DM $\rho_{AA}^{(0)}$.

Atomic weight functions used to partition the electron density (e.g., from an iterative-Hirshfeld analysis) can be transformed to trial weight matrices $w_A^{(0)}$ in a finite basis set.[12] However, these atomic weight functions pick up non-negligible contributions from core electrons and free electron pairs on other atoms (since there is no orbital selectivity), and this characteristic might be inherited throughout the orthogonalization procedure.

Therefore, when the SPA method was introduced,[15] the atomic 1DMs of isolated atoms were used as the starting points. However, different results are obtained depending on the charge and electronic state of the isolated atom (similar to the case of the standard Hirshfeld method[6]). As an example, the partial charge on the Na atom in NaCl (with a B3LYP/aug-cc-pVDZ geometry and a 1DM calculated at the RHF/aug-cc-pVDZ level) is +0.89 when the orthogonalization procedure is started from the neutral atoms, but amounts to +0.98 when the ions are chosen as starting points. To eliminate this arbitrariness, the optimal charges and states of the trial atoms are required to be consistent with the charges and orbital populations of the final atoms (that have a 1DM $\rho_{AA}^{(\infty)}$). In close analogy to the iterative-Hirshfeld procedure,[6–9] the consistency requirement is implemented through an outer iterative loop. After convergence of the inner (orthogonalization) loop, the orbital populations $n_{AA,k}^{(\infty)}$ of the atomic 1DM $\rho_{AA}^{(\infty)}$,

$$\rho_{AA}^{(\infty)} = \sum_k n_{AA,k}^{(\infty)} \varphi_{AA,k}^{(\infty)} \left(\varphi_{AA,k}^{(\infty)}\right)^T, \quad (9)$$

are obtained by diagonalization of $\rho_{AA}^{(\infty)}$. The $\varphi_{AA,k}^{(\infty)}$ are column matrices and represent the eigenvectors. These orbital populations are then used to construct a new starting point for the inner loop,

$$\rho_{AA}^{(0)*}[N_A] = \sum_l n_{AA,l}^{(\infty)} \varphi_{AA,l}^{(0)} \left(\varphi_{AA,l}^{(0)}\right)^T, \quad (10)$$

where $\varphi_{AA,l}^{(0)}$ represents an orbital (eigenvector) of a charged isolated atom 1DM determined as a linear interpolation between the 1DMs of the atoms with integer electron numbers:[25–27]

$$\rho_{AA}^{(0)}[N_A] = (k + 1 - N_A)\rho_{AA}^{(0)}[k] + (N_A - k)\rho_{AA}^{(0)}[k+1]. \quad (11)$$

Note that the matrix on the left side of Eq. (10) has the same eigenvectors as the isolated atom 1DM of Eq. (11), but with occupations that reflect the molecular environment.

The procedure for establishing the correspondence between the orbitals of $\rho_{AA}^{(\infty)}$ and $\rho_{AA}^{(0)}(N_A)$ is based on the principle of maximal orbital overlap. The 1DM $\rho_{AA}^{(\infty)}$ is expressed in the basis of the molecular orbitals. $\rho_{AA}^{(0)}(N_A)$ is calculated (and rotationally averaged) in a smaller atomic basis, and then extended to the same molecular orbital basis. At first sight, an unambiguous correspondence is only evident when there is a high similarity between both sets of orbitals and when these orbitals are properly oriented. To create a unique correspondence when both sets of orbitals are less similar, we introduce matrices that are intermediate (i.e., interpolated) between $\rho_{AA}^{(\infty)}$ and $\rho_{AA}^{(0)}[N_A]$. When the intermediate matrix has a dominant contribution of $\rho_{AA}^{(\infty)}$, then the overlap of each of its orbitals with each of the orbitals $\varphi_{AA}^{(\infty)}$ is arbitrarily close to either 1 or 0. For an intermediate matrix that has a dominant contribution of $\rho_{AA}^{(0)}[N_A]$, the overlap of each of its orbitals with each of the orbitals $\varphi_{AA}^{(0)}$ is arbitrarily close to either 1 or 0. A successive transfer of populations from the orbitals $\varphi_{AA}^{(\infty)}$ to the orbitals of the intermediate matrices, and finally to the orbitals of the isolated atom $\varphi_{AA}^{(0)}$, is needed to construct $\rho_{AA}^{(0)*}(N_A)$ in an unambiguous manner. It must be noted that in most cases only a few intermediate matrices (one or two) are needed to fix the correspondence of the orbitals.

In Ref. 15, we also introduced a less sophisticated outer loop procedure called the "charge equalization scheme." Here, only the atomic charges of rotationally averaged atomic 1DMs $\rho_{AA}^{(0)}$ were adjusted during successive iterations of the outer loop (i.e., Eq. (11) was used as a starting point for the inner loops). In the present paper we only present calculations with the full procedure described in Eqs. (9)–(11), called the "population equalization scheme" in Ref. 15, as we find that

the results are markedly superior especially in cases where the orbital orientations play an important role. In this case Eq. (10), rather than Eq. (11), determines the starting point of the inner loops.

The choice of starting point determines not only the chemical relevance of the scheme, but also the preference for the matrix M in Eqs. (7) and (8). When the trial weight matrices are nearly orthogonal, then $M = \rho$ appears to be the most elegant choice in Eqs. (7) and (8) (see Sec. VI B). This is the case when the trial weight matrices are based on the 1DMs of isolated atoms,[15] as is done in this paper. When the trial weight matrices are further from orthogonality (e.g., the Hirshfeld-I weight matrices) then it may be safer to use $M = \rho^{(i-1)}$ in order to guarantee that the scheme converges to a set of orthogonal weight matrices and to avoid particular nonorthogonal solutions that can be reached if $M = \rho$.

IV. INTERPRETATIVE ADVANTAGES OF PARTITIONING WITH ORTHOGONAL PROJECTORS

A. Non-bonded atoms

1DM partitioning with orthogonal projectors facilitates considerably the interpretation of the atomic and bond matrices. It was already mentioned that the ρ_{AA} can be regarded as 1DMs of atoms that are excited by the molecular environment without loss of electrons to the bonds (Eq. (5)). The bond matrices describe the electronic rearrangements that occur when a covalent bond is formed between atoms A and B. From Eq. (4), it is clear that upon convergence no electrons are shared between different atomic matrices $\rho_{AA}^{(\infty)}$:

$$Tr\left(\rho_{AA}^{(\infty)}\rho_{BB}^{(\infty)}\right) = Tr\left(\left(\rho_{AA}^{(\infty)}\right)^2\right)\delta_{AB}. \tag{12}$$

Since the sharing of electrons between the atoms in a molecule is identified with the process of chemical bonding, Eq. (12) is the basis for the interpretation of $\rho_{AA}^{(\infty)}$ as the 1DM of a "non-bonded" atom in a molecular environment. Note that this interpretation holds here for the normal molecular geometry, and has nothing to do with dissociation processes. Also, no contributions of the $\rho_{AA}^{(\infty)}$ can be assigned to atom pairs,

$$w_B^{(\infty)}\left(\rho_{AA}^{(\infty)}\right)w_C^{(\infty)} = \rho_{AA}^{(\infty)}\delta_{AB}\delta_{AC}. \tag{13}$$

Only when orthogonal projectors are used for the 1DM-partitioning, Eqs. (12) and (13) are trivially satisfied.

B. Bonded atoms

A very different interpretation is attached to the single-index atomic 1DM's $\rho_A^{(\infty)}$, that are derived by single insertion of the converged orthogonal weight matrices $w_A^{(\infty)}$ into the molecular 1DM,

$$\rho_A^{(\infty)} = \rho^{\frac{1}{2}} w_A^{(\infty)} \rho^{\frac{1}{2}}, \quad \sum_A \rho_A^{(\infty)} = \rho. \tag{14}$$

In contrast to the double-index atomic matrices $\rho_{AA}^{(\infty)}$, these N-representable matrices do share electrons. The number of electrons that is shared between the single-index atoms is equivalent to the number of electrons shared by the bond matrices:

$$Tr\left(\rho_A^{(\infty)}\rho_B^{(\infty)}\right) = Tr\left(\rho_{AB}^{(\infty)}\rho\right) = 2Tr\left(\rho_{AB}^{(\infty)}\rho_{BA}^{(\infty)}\right) \neq 0. \tag{15}$$

Therefore, the single-index atomic matrices $\rho_A^{(\infty)}$ can be considered as effectively "bonded" within the molecular geometry. The property in Eq. (15) is only trivially satisfied when orthogonal projectors are used.

C. Electron delocalization in "bonded" and "non-bonded" atoms

There are intimate connections between the single-atom (Eq. (14)) and double-atom 1DMs (Eq. (2)). Defining $C = \rho^{\frac{1}{2}} w_A^{(\infty)}$, one can rewrite

$$\begin{aligned} \rho_A^{(\infty)} &= CC^T, \\ \rho_{AA}^{(\infty)} &= C^T C, \end{aligned} \tag{16}$$

which implies that both sets of 1DMs share the same eigenvalue spectrum. Numerical evidence suggests that while the orbitals of the double-atom 1DMs are localized, the orbitals of the single-atom 1DM atoms have the shape of typical molecular orbitals (e.g., σ and π). This is consistent with the

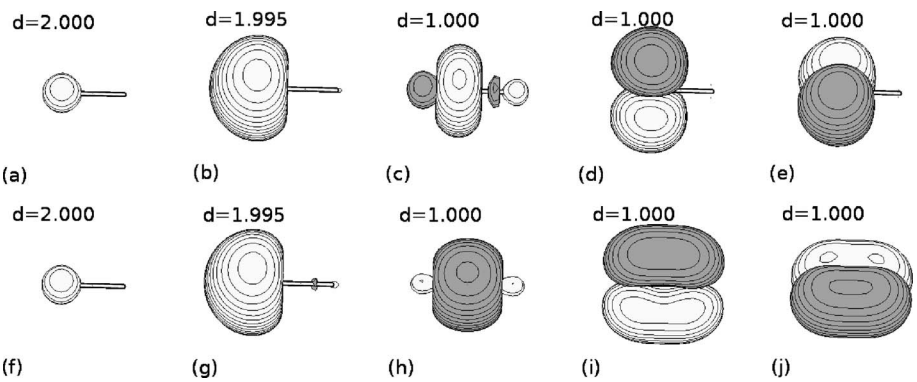

FIG. 1. Dominant natural orbitals and populations of the "non-bonded" $\rho_{AA}^{(\infty)}$ (a-e) and the "bonded" $\rho_A^{(\infty)}$ (f-j) in a N_2 molecule at the RHF/aug-cc-pVDZ level of theory. The isosurface value (in a.u.) used is $\pm$ 0.1.

interpretation of "non-bonded" and "bonded" atoms in the molecule. As an example, Fig. 1 displays the main orbitals of the single-atom and double-atom 1DMs of N_2.

As noted in Ref. 12, any single-atom 1DM definition suffers from bad localization properties. For the "bonded" single-atom 1DMs in Eq. (14), the population d_i of a natural orbital φ_i in the molecular 1DM is simply divided over the occupancies $d_{A,i}$ for that orbital in the single-atom 1DMs:

$$d_{A,i} = \left(\rho_A^{(\infty)}\right)_{ii} = d_i \langle \varphi_i | w_A^{(\infty)} | \varphi_i \rangle,$$
$$\sum_A d_{A,i} = d_i. \tag{17}$$

This implies that only orbitals φ_i that are occupied in the molecule are also occupied in the atoms. Typical chemical compounds have large populations for the bonding orbitals and smaller populations for the antibonding orbitals. Since good localization properties for the atoms are obtained only if the bonding and antibonding molecular orbitals have about equal occupancies in the atom, we conclude that the degree of electron delocalization in the single-index atoms is similar to the degree of electron delocalization in the molecule.

In contrast, the double-index atoms in Eq. (2) have good localization properties. The occupancy $d_{AA,i}$ of each (bonding and antibonding) molecular orbital φ_i in the double-atom 1DMs gets contributions from all populations in the molecular 1DM:

$$d_{AA,i} = \left(\rho_{AA}^{(\infty)}\right)_{ii} = \sum_k d_k \langle \varphi_i | w_A^{(\infty)} | \varphi_k \rangle^2. \tag{18}$$

Therefore, similar occupancies are obtained for bonding and antibonding molecular orbitals. This results in excellent localization properties for the orbitals of $\rho_{AA}^{(\infty)}$, as is clear from Figs. 1(a)–1(e). However, small orthogonalization tails can be observed in some cases, e.g., in the p_z orbital on N (Fig. 1(c)).

Fig. 2 illustrates the localization properties of the fragments of the molecular electron density (the diagonal of the 1DM) for the N_2 molecule at the RHF/aug-cc-pVDZ level. $\rho_{AA}^{(\infty)}(\boldsymbol{r})$ is clearly local and positive-semidefinite. $\rho_{AB}^{(\infty)}(\boldsymbol{r})$ has negative and positive contributions, and reflects a shift of the electron density from the atomic regions to the bonding region. The single-atom $\rho_A^{(\infty)}(\boldsymbol{r})$ is heavily delocalized.

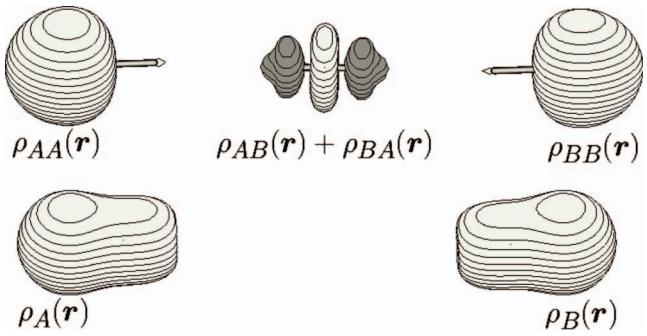

FIG. 2. Localization properties of the fragments of the molecular electron density (the diagonal of the 1DM) for the N_2 molecule at the RHF/aug-cc-pVDZ level. The isosurface value (in a.u.) used is ± 0.1.

D. Bond orders and bond polarization

At the Hartree-Fock level, the quantum mechanical bond order index (also shared-electron distribution index)[28–37] is determined from the integration of the exchange density over atomic domains:

$$B_{AB} = \frac{1}{2} \int d\boldsymbol{r} d\boldsymbol{r}' w_A(\boldsymbol{r}) \rho(\boldsymbol{r}, \boldsymbol{r}') w_B(\boldsymbol{r}') \rho(\boldsymbol{r}', \boldsymbol{r}). \tag{19}$$

Note that this expression applies to closed-shell single-determinant wave functions. The atomic weight functions $w_A(\boldsymbol{r})$ in Eq. (19) are a special case of the more general atomic weight matrices $w_A(\boldsymbol{r}, \boldsymbol{r}')$ used in this paper, in a sense that they are diagonal in $\boldsymbol{r}$-space. These quantities, that obey the property $\sum_A w_A(\boldsymbol{r}) = 1$, are used extensively in the AIM literature that is concerned with the partitioning of the electron density $\rho(\boldsymbol{r})$ in $\boldsymbol{r}$-space. In Eq. (19), atomic weight functions $w_A(\boldsymbol{r})$ can be taken from any particular AIM model (e.g., the Hirshfeld-I model, see Table IV in Sec. VI). In the SPA-framework, the definition in Eq. (19) can be extended to general atomic weight matrices (that are not diagonal in $\boldsymbol{r}$-space), as

$$B_{AB}^{(SPA)} = \frac{1}{2} Tr\left(\rho_A^{(\infty)} \rho_B^{(\infty)}\right) = Tr\left(\rho_{AB}^{(\infty)} \rho_{AB}^{(\infty)}\right). \tag{20}$$

One can easily show that Eq. (20) reduces to Eq. (19) if the weight matrices are diagonal in $\boldsymbol{r}$-space, and that it is invariant under unitary transformations. Note that Eq. (20) is not related to the concept of overlap populations, defined as $\int d\boldsymbol{r} w_A(\boldsymbol{r}) \rho(\boldsymbol{r}) w_B(\boldsymbol{r})$. Extending to general weight matrices this would become $Tr(\rho_{AB})$, which is zero in the SPA framework.

It appears that within the framework of orthogonal projectors, the covalent bond order can be identified with Eq. (20) and is just the number of electron pairs shared between bonded atoms (or bond matrices). Since this seems to be a very natural statement for the quantum mechanical bond-order index, we propose to use Eq. (20) to assess the covalent bond order also at the post-Hartree-Fock level.

For homonuclear diatomic molecules calculated at the Hartree-Fock level, Eq. (20) is extremely close to the classical bond order, as could be expected from Fig. 1. The deformation matrices $\Delta\rho_A^{(\infty)}$ that transform the "non-bonded" atoms $\rho_{AA}^{(\infty)}$ into the corresponding "bonded" atoms $\rho_A^{(\infty)}$,

$$\Delta\rho_A^{(\infty)} = \rho_A^{(\infty)} - \rho_{AA}^{(\infty)}, \tag{21}$$

are traceless and in addition may be considered to be atom-condensed bond matrices:

$$\sum_A \Delta\rho_A^{(\infty)} = \sum_{A,B \neq A} \rho_{AB}^{(\infty)}. \tag{22}$$

Using these atom-condensed bond matrices, it is possible to define the contribution of atom A to the covalent AB bond order as

$$B_{A_{(B)}}^{(SPA)} = \frac{1}{2} Tr\left(\Delta\rho_A^{(\infty)} \rho_{AB}^{(\infty)}\right). \tag{23}$$

In case of a diatomic, it is easy to see (using the orthogonal projector relationship) that

$$B_{AB}^{(SPA)} = Tr\left(\rho_{AB}^{(\infty)}\rho_{AB}^{(\infty)}\right) = \frac{1}{2}Tr\left(\left(\Delta\rho_{A}^{(\infty)} + \Delta\rho_{B}^{(\infty)}\right)\rho_{AB}^{(\infty)}\right)$$
$$= B_{A_{(B)}}^{(SPA)} + B_{B_{(A)}}^{(SPA)}. \quad (24)$$

Numerically, we found that Eq. (24) is also satisfied in the general case. We refer to the Sec. VI for more details. From Eq. (23), it is possible to assess the share of each atom in the creation of the bond. Classical chemistry distinguishes between normal covalent bonding and dative covalent bonding when a bond is formed between neutral atoms. In a normal covalent bond, each atom has an equal share in the bond order. In a dative covalent bond, only one atom provides the electrons for bonding. In the ABIM framework, a bond is formed between partially charged atoms and covalent bonds display a continuous spectrum between "normal" and "dative" bonding. From the splitting of the bond order in Eq. (24), it is then possible to assess the "normal" and "dative" character of the covalent bond.

V. COMPARISON WITH NATURAL POPULATION ANALYSIS

The notion of using orthogonal projectors in a double-atom partitioning scheme for the 1DM is reminiscent of the natural population analysis (NPA) (Ref. 21) introduced by Reed *et al.* in 1985. In NPA, blocks of the 1DM are considered on the basis of the attachment of basis functions to the atomic centers. An orthogonal basis is constructed that, at least for orbitals corresponding to a minimal basis set, remain very close to the original atom-centered nonorthogonal basis functions. When the density matrix is expressed in this orthogonal basis, the blocks on the diagonal (AA and BB) can be considered to be orthogonal atomic fragments of the density matrix and the off-diagonal blocks (AB and BA) are the bond fragments. The bond fragments are traceless and their eigenvalues come in pairs with opposite signs.[20] This is very similar to the SPA double-atom partitioning of the density matrix, based on orthogonal atomic weight matrices.

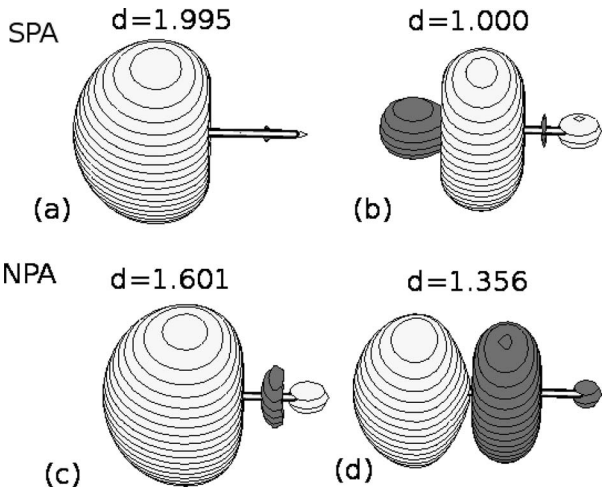

FIG. 3. Typical differences between the eigenfunctions of $\rho_{AA}^{(\infty)}$ in the new SPA method and the natural atomic orbitals in NPA. For a N_2 molecule at the RHF/aug-cc-pVDZ level, the 2s and $2p_z$ orbitals on the first N atom obtained using SPA ((a) and (b)) are compared to their counterparts in NPA ((c) and (d)). The differences between the 1s, $2p_x$ and $2p_y$ orbitals are rather small. The isosurface value (in a.u.) used is $\pm$ 0.1.

Both approaches, however, are not equivalent. As an example, Fig. 3 displays typical differences found between the eigenfunctions of $\rho_{AA}^{(\infty)}$ in the SPA method and the natural atomic orbitals of the (AA) block in NPA. The example is chosen so that the result is not influenced by the choice of the outer loop in SPA (N_2 has zero atomic charges and equal populations for the p orbitals). Any differences observed between both methods reflect only the orthogonalization procedure. In NPA, the orthogonalization procedure is constructed so as to maintain a maximal similarity for a minimal basis set to the original atom-centered basis functions. Therefore the 2s and p_z orbitals in N_2 (see Figs. 3(c) and 3(d)) are the slightly deformed versions of the atom-centered basis functions. In contrast to the Mulliken procedure, NPA converges rather well with increasing basis set, although one could argue that the original atom-centered orbitals play a preferential role. In SPA, the 2s and p_z orbitals (see Figs. 3(a) and 3(b)) are equally well localized, but they reflect more the actual electronic orbitals in the molecule. The 2s orbital is shifted outwards to accommodate the free electron pair (it has a population of 1.995) and the $2p_z$ orbital resembles a fragment of the molecular σ orbital (with population 1.000). The corresponding populations in NPA are very different (1.601 and 1.356 respectively). The differences between both methods in the shape and occupancies of the 1s, $2p_x$, and $2p_y$ orbitals are rather small.

The SPA orthogonalization procedure seems, in our view, more straightforward than the NPA one. In NPA, a block structure of the molecular 1DM is identified based on the atom attachment of the basis functions. These blocks are rotationally averaged and diagonalized to obtain a first approximation to the Natural Atomic Orbitals (pre-NAOs). In a second step, the pre-NAOs are classified as belonging to the "minimal basis set" or the "Rydberg basis set" (that consists of leftover functions). Then, a complicated sequence of orthogonalization procedures follows aiming at preserving the atomic character of the minimal basis set. In the SPA procedure, the atomic weight projectors are orthogonalized through a simple iterative self-consistency loop. No distinction is made between different types of orbitals. The final shape of the atomic orbitals is based on the isolated-atom 1DMs used as a starting point of the iterative procedure, but also reflects the molecular environment. Note that the outer loop in SPA only provides suitable starting points for the orthogonalization procedure in the inner loop, and could even be avoided if some set of nonorthogonal weight matrices from alternative approaches are used as a starting point.

VI. RESULTS

A. Computational methods

For the SPA method described in Ref. 15 and in Secs. II and III, numerical tests were performed on the recursive scheme used to construct orthogonal projectors. The molecular 1DMs used in these tests originated from a small set of ca. 67 simple molecules representative of a variety of

TABLE I. List of molecules in the test set.

$AlCl_3$	C_4H_4	CH_3F	CO	$HCOOCH_3$	LiOH	P_2
AlH_3	C_4H_6	CH_3NH_2	CO_2	HF	N_2	P_2H_4
B_2H_6	C_6H_6	CH_3OCH_3	F_2	HNO_2	N_2H_2	PH_3
BeH_2	CCl_4	CH_3OH	H_2	HNO_3	N_2O	S_2
BH_3	CF_4	CH_4	H_2O	HOCl	NaCl	SF_6
C_2H_2	CH_2F_2	CHF_3	H_2S	HOOH	NaOH	Si_2H_6
C_2H_4	CH_2NH	$CHONH_2$	H_2SO_4	HSSH	NH_3	SiH_4
C_2H_6	CH_2O	CHOOH	H_3O^+	Li_2	O_2	
C_3H_3N	CH_2O_2	Cl_2	HCl	LiF	O_3	
C_3H_4	$CH_3CH_2CH_3$	ClF_3	HCN	LiH	OS_2	

chemical bonds. The list of molecules, which was also used in Ref. 15 is presented in Table I. All molecules have a singlet ground-state, apart from O_2, for which we consider the singlet (excited) state. Molecular geometries were obtained from a B3LYP (Refs. 38–41) /cc-pVDZ (Refs. 42–44) optimization. The molecular 1DMs were calculated at the restricted Hartree-Fock level of theory using the aug-cc-pVDZ basis set.[42,45] To eliminate the starting-point dependence of the 1DM partitioning scheme, self-consistency was enforced for the populations of the atomic orbitals as outlined in Sec. III and Ref. 15.

To assess the interpretative advantages associated with the use of orthogonal projectors for the 1DM partitioning, we also calculated covalent bond orders for a small subset of mainly diatomic molecules. For that purpose additional calculations were performed at the full-valence CASSCF level of theory, for varying bond lengths.

B. Orthogonal projectors from a stockholder approach: numerical evidence

In the preceding theoretical discussion, it was assumed that the weight matrices obtained from the recursive scheme in Eq. (7) are orthogonal projectors. It was shown that this should be inevitably the case when $M = \rho^{(i-1)}$. However, for the more elegant implementation of the recursive scheme (when $M = \rho$) , we were unable to prove that the resulting weight matrices are indeed binary, since orthogonal projectors are only a subset of the entire solution set.

Numerical results seem to indicate that the recursive scheme with $M = \rho$ outcompetes the implementation with $M = \rho^{(i-1)}$, when the starting points are close to orthogonal projectors. In Fig. 4 the numerical accuracy is shown for the relationship that defines orthogonal projectors (in terms of the converged weight matrices). For each molecule in the entire test set, all atom pairs AB contribute to a matrix C_{AB} that reduces to the zero matrix for perfect orthogonal projectors:

$$C^{(1)}_{AB} = w^{(\infty)}_A w^{(\infty)}_B - \delta_{AB} w^{(\infty)}_A. \tag{25}$$

The matrix element with a maximal deviation from zero in C_{AB}, for all atom pairs, is chosen to represent the accuracy obtained for that molecule. A histogram is created from the integer logarithms of these accuracy measures.

When $M = \rho$ in Eq. (7), we indeed find that the relationship associated with orthogonal projectors is extremely well fulfilled by the weight matrices from the recursive scheme (the largest nonzero element of the C_{AB} matrices being smaller than 10^{-8}). Note that the accuracy limit (10^{-8}) is determined by the convergence criterion and this limit can be shifted to smaller values by requiring a more tight convergence. Therefore, we consider it as proven that even with this implementation (for which there is no airtight theoretical proof) the initial weight matrices are transformed into perfect orthogonal projectors for every molecule in the test set. For the alternative implementation of the recursive scheme (where $M = \rho^{(i-1)}$), it is observed that for only half of the molecules in the test set the largest nonzero element of the C_{AB} matrices is smaller than 10^{-5}. There are even cases for which an element larger than 10^{-1} was found, which is seemingly in contrast to the theoretical prediction that for this implementation all the obtained weight matrices should be orthogonal projectors. The analytical proof, however, assumes that in Eq. (7) the matrix $\rho^{(i)}$ can be inverted. Since we started from Hartree-Fock 1DMs of the isolated atoms and of the molecule, nullspace will inevitably be present in these matrices. We have replaced zero eigenvalues in $\rho^{(0)}_{AA}$ with a small value of 10^{-5} in order to avoid this, an operation which has no effect on the final fragments $\rho^{(\infty)}_{AA}$. For $M = \rho$ this is sufficient to remove nullspace issues during the iterations. The $M = \rho^{(i-1)}$ scheme, however, is less stable in this respect and the matrices become close to singular during successive iterations. We checked that the stability of the latter scheme is enhanced when small eigenvalues in $\rho^{(0)}_{AA}$ are replaced with a somewhat larger value of 10^{-3}. In that case, there is a drastic improvement of the accuracy values (which become consistently smaller than 10^{-8} for all molecules), although this operation has a small effect on the final fragments. It shows that the stability problem in this scheme is just a numerical issue that disappears when there are no (near) nullspaces in $\rho^{(i-1)}_{AA}$.

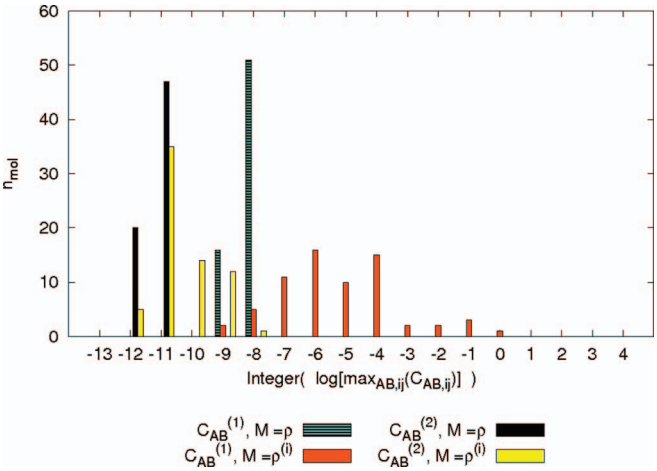

FIG. 4. Attained numerical accuracy in obtaining weight matrices that are orthogonal projectors, through the use of the recursive scheme. For details, see text.

Multiplying Eq. (25) on both sides with $(\rho^{(\infty)})^{+\frac{1}{2}}$, one obtains

$$C^{(2)}_{AB} = \rho^{(\infty)}_{AA} \left(\rho^{(\infty)}\right)^{-\frac{1}{2}} \rho^{(\infty)}_{BB} - \delta_{AB} \rho^{(\infty)}_{AA}, \tag{26}$$

where $\rho^{(\infty)}_{AA}$ is a shorthand notation for the converged matrix $w^{(\infty)}_A M w^{(\infty)}_A$. Expression (26) is an equivalent orthogonal-projector relationship, but is restricted to the relevant or

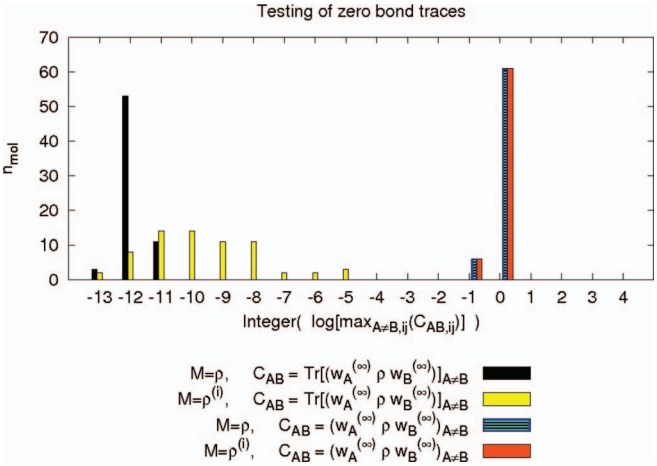

FIG. 5. Attained numerical accuracy in obtaining nonzero bond matrices with a zero trace.

"occupied" part of space. It is clear from Fig. 4 that the weight matrices from both recursive schemes satisfy these relationships almost perfectly (the largest nonzero element of the C_{AB} matrices being consistently smaller than 10^{-8}). This observation confirms that both schemes construct perfect orthogonal projectors for the relevant subspace.

In Fig. 5, we examined which accuracy was obtained for the zero bond traces, a direct consequence of the use of orthogonal projectors. For each molecule in the test set, the largest bond trace is smaller than 10^{-11} when $M = \rho$, and smaller than 10^{-5} when $M = \rho^{(i-1)}$. The implementation with $M = \rho$ performs consistently better, which is again tied to the nullspace issue. To show that there are considerable bond matrices for all molecules in the test set (also for the ionic compounds), the largest element in the bond matrices is also presented. There is no molecule for which all bond matrix elements are smaller than 10^{-2}.

In the current analysis, the 1DMs of isolated atoms provide the starting points of the iterative scheme. In this case, the standard recursive scheme (where $M = \rho$) is superior since it is more elegant and less prone to numerical problems. On the other hand, the alternative recursive scheme (where $M = \rho^{(i-1)}$) could be useful if, e.g., the iterative Hirshfeld weight matrices would be chosen as the starting point for the iterations. The iterative-Hirshfeld weight matrices (as used in Ref. 12) are not close to a set of orthogonal projectors. As a result, the standard scheme might converge to a nonorthogonal solution, while such an event is excluded in the alternative scheme (see Sec. II).

C. Interpretative advantages: Transferability of the atoms and bonds

An approximate transferability of atoms and bonds in molecules across similar compounds is a necessary criterion for any ABIM approach. For techniques based on a partitioning of the molecular electron density over atoms, it is widely recognized that transferability requires local atomic electron densities. For density-matrix based approaches, localization is a more subtle issue. It is easy to understand (see, e.g., Ref. 12) that a fragment $\rho_A(\boldsymbol{r}, \boldsymbol{r}')$ in any single-atom partitioning scheme of the molecular 1DM cannot be localized to the atomic region of A.

For a general double-atom partitioning of the molecular density matrix, as introduced in Eq. (2), several situations can be considered. When the weight matrices w_A are diagonal in $\boldsymbol{r}$ space, $\rho_{AB}(\boldsymbol{r}, \boldsymbol{r}')$ can be localized to the atom pair AB, provided local weight functions $w_A(\boldsymbol{r})$ and $w_B(\boldsymbol{r})$ are used. If these weight functions are also binary (as in QTAIM, i.e., $w_A(\boldsymbol{r}) = \chi_A(\boldsymbol{r}) = 0/1$ if $\boldsymbol{r}$ is outside/inside the domain of atom A), and therefore orthogonal projectors satisfying Eq. (4), then the corresponding atomic 1DM fragments do not have tails that stretch into the domains of other atoms,

$$\rho_{AA}^{QTAIM}(\boldsymbol{r}, \boldsymbol{r}') = \sum_i d_i(\chi_A(\boldsymbol{r})\varphi_i(\boldsymbol{r}))(\chi_A(\boldsymbol{r}')\varphi_i(\boldsymbol{r}')). \quad (27)$$

In Eq. (27), $\varphi_i(\boldsymbol{r})$ and d_i represent a molecular orbital and its population.

In the SPA framework, the orthogonal projectors w_A are not diagonal in $\boldsymbol{r}$ space and small "orthogonalization" tails

TABLE II. Populations in ρ_{AA} are quite transferable to similar compounds. The first line indicates the valence orbitals in isolated atoms ($2s,2p_x,2p_y,2p_z$). The second line indicates the type of bond these are prepared to form in the molecule (lp = lone pair, X = a heteroatom), according to the deformations of ρ_{AA}. The following lines list the populations of the orbitals of ρ_{AA} in similar compounds, at the RHF/aug-cc-pVDZ level.

$\rho_{CC}(CH_3)$	2s C-H	$2p_x$ C-H	$2p_y$ C-H	$2p_z$ C-X	$\rho_{OO}(OH)$	2s lp	$2p_x$ lp	$2p_y$ O-H	$2p_z$ O-X
CH_3H	1.18	1.22	1.22	1.22	HOOH	2.00	1.99	1.60	0.99
CH_3CH_3	1.12	1.21	1.21	0.99	HOCl	2.00	1.99	1.62	1.18
CH_3NH_2	1.09	1.17	1.22	0.75	CH_3OH	1.98	1.96	1.59	1.40
CH_3OH	1.09	1.17	1.21	0.57	HCOOH	1.99	1.90	1.62	1.42
CH_3F	1.11	1.22	1.22	0.43	HOH	2.00	1.98	1.64	1.57
CH_3Cl	1.20	1.28	1.28	0.71	LiOH	1.98	1.98	1.59	1.58
$\rho_{OO}(CO)$	2s lp	$2p_x$ lp	$2p_y$ $C{=}O_{(\pi)}$	$2p_z$ $C{=}O_{(\sigma)}$	$\rho_{CC}(CO)$	2s C-H	$2p_x$ $C{=}O_{(\pi)}$	$2p_y$ $C{=}O_{(\sigma)}$	$2p_z$ C-X
HCOH	1.99	1.89	1.41	1.35	HCOH	1.11	0.58	0.64	1.13
$HCOOCH_3$	1.99	1.88	1.54	1.30	$HCOOCH_3$	1.04	0.54	0.70	0.54
HCOOH	1.99	1.88	1.57	1.34	HCOOH	1.06	0.51	0.66	0.57
$HCONH_2$	1.99	1.89	1.60	1.32	$HCONH_2$	1.05	0.53	0.62	0.77

TABLE III. Transferability of the bond orders $B_{AB}^{(SPA)}$ to similar compounds at the RHF/aug-cc-pVDZ level.

	CH_4	CH_3CH_3	CH_2CH_2	CH_3NH_2	CH_3OH	CH_2O	CHF_3	CHOOH	HCN	CHCH
$B_{CH}^{(SPA)}$	0.95	0.95	0.94	0.95	0.95	0.95	0.94	0.93	0.93	0.87
	H_2O	HOOH	CH_3OH	HCOOH	LiOH	HOCl				
$B_{OH}^{(SPA)}$	0.65	0.61	0.64	0.61	0.64	0.62				
	NH_3	N_2H_2	CH_3NH_2	CH_2NH	$CHONH_2$					
$B_{NH}^{(SPA)}$	0.83	0.82	0.79	0.79	0.75					
	H_2CO	HCOOH	$HCOOCH_3$	$HCONH_2$						
$B_{C=O}^{(SPA)}$	1.83	1.65	1.65	1.60						
	C_2H_4	C_3H_4	C_4H_6							
$B_{C=C}^{(SPA)}$	2.01	1.94	1.91							

may appear on neighboring atoms (just as in NPA), as can be inferred from Fig. 3 (b). However, these small tails have little impact on the transferability of the atomic fragments. This could already be expected from the excellent linear correlation of the atomic charges in the new SPA method with the atomic charges from a Hirshfeld-I AIM model.[15] A more elaborate investigation is presented in Table II, that assesses the transferability of some functional groups (CH_3, OH, and CO) within a wide range of chemical compounds. This assessment is focussed on the orbital populations of ρ_{AA}. It appears that significant differences only appear in the orbital that attaches the functional group to the molecule (C-X, O-X and C-X). The populations of free electron pairs and of orbitals pointed towards the other atoms of the functional group are remarkably constant. Transferability is of course important, but the main goal of this scheme is to investigate the differences rather than the similarities between molecules, e.g., the effect that electron delocalization in conjugated π systems has on the orbital occupancies. One can infer from Table II that an increased degree of conjugation (e.g., in $HCONH_2$) boosts the population of the p-orbital on O in CO that is involved in this conjugated π system.

Let us now consider the transferability of the 1DM fragments associated with the bonds (ρ_{AB}, A $\neq$ B). Table III addresses the transferability of some bonds (CH, OH, NH, C=C, C=O) within a wide range of chemical compounds. This assessment is focussed on the covalent bond orders $B_{AB}^{(SPA)}$. Again, these bond orders are remarkably constant in different compounds. It is interesting to investigate the effect of π conjugation in some systems on the bond orders. One can infer from Table III that an increased degree of conjugation (e.g., in $HCONH_2$) suppresses the C=O bond order in molecules with a carbonyl functional group. In Sec. VI D, we elaborate on these covalent bond orders.

D. Interpretative advantages: examination of covalent bond orders

Hartree-Fock covalent bond orders are trivial in many cases (e.g., homonuclear diatomic molecules), and their reproduction is an excellent test for any ABIM scheme. In Table IV, the number of electron pairs shared between "bonded atoms" $B_{AB}^{(SPA)}$ (Eq. (20)) is compared to the well-established Hirshfeld-I SEDI-index $B_{AB}^{(HI)}$ at the Hartree-Fock level of theory. For homonuclear diatomic molecules, it is confirmed that values for $B_{AB}^{(SPA)}$ are quite close to the integer values of the classical bond orders. In particular for the halogen gases, the expected values are obtained. For the Hirshfeld-I AIM model, values obtained for the SEDI-index in these molecules are clearly larger than dictated by intuition and would seem to indicate that the "free electron pairs" contribute to the bond order. Note that this is a defect of the Hirshfeld-I AIM model, not of the SEDI-index. For ionic compounds, it is satisfying to observe that covalent bond orders in the orthogonal projector framework deviate only a few percent (0.03–0.08) from zero. Hirshfeld-I SEDI-indices for these compounds are much larger (0.26–0.32). For polar covalent compounds, values for the bond order indices are inversely correlated with the charges on the atoms.

In Table V, the contribution of the individual atoms to the bond (order) is examined (see Eq. (23)). Relative contributions are presented as $x_{(AB)}^{A} = B_{A_{(B)}}^{(SPA)} / B_{AB}^{(SPA)}$. The values for $x_{(AB)}^{A}$ indicate that in the ABIM framework, the atoms do not contribute equally to the covalent bond. The contribution is mainly determined by the atomic charge and can be approximated (in the diatomic case) with the simple formula:

$$x_{(AB)}^{'A} = \frac{((b.o.)_{AB} - Q_A + F_A)}{2(b.o.)_{AB}}, \tag{28}$$

where $(b.o.)_{AB}$ is the classical number of bonds between the atoms (covalent or ionic), Q_A is the atomic charge determined from the AIM and F_A is the formal charge. Note that for zero charges on the atoms, the classical number of dative bonds is obtained as $|x_{(AB)}^{'A} - x_{(AB)}^{'B}|(b.o.)_{AB}$.

TABLE IV. Comparison of the covalent bond orders obtained in the orthogonal projector framework ($B_{AB}^{(SPA)}$) with the well established iterative-Hirshfeld SEDI-index ($B_{AB}^{(HI)}$). Values, calculated at the RHF/aug-cc-pVDZ level, are shown for the diatomic molecules in the test set.

	$B_{AB}^{(HI)}$	$B_{AB}^{(SPA)}$		$B_{AB}^{(HI)}$	$B_{AB}^{(SPA)}$
H_2	1.00	1.00	LiH	0.26	0.08
F_2	1.58	1.01	LiF	0.26	0.05
Cl_2	1.75	1.04	NaCl	0.32	0.03
Li_2	1.03	1.00	HF	0.80	0.48
O_2	2.69	2.02	CO	2.84	2.15
N_2	3.33	3.02	HCl	1.12	0.91
S_2	2.77	2.04	H_2O	0.88	0.65
P_2	3.29	3.01			

TABLE V. The contribution of the individual atoms to the covalent bond, for the diatomic molecules in the test set calculated at the Hartree-Fock level. The covalent bond order $B_{AB}^{(SPA)}$ and its relative contributions from the atoms ($x_{(AB)}^{A}$ and $x_{(AB)}^{B}$) are determined within the orthogonal projector framework. Note that $x_{(AB)}^{A} + x_{(AB)}^{B} = 1$. The relative atomic contributions can also be estimated with a simple formula ($x_{(AB)}^{'A}$ and $x_{(AB)}^{'B}$) from the atomic charges Q_A.

	Q_A	Q_B	$B_{AB}^{(SPA)}$	$x_{(AB)}^{A}$	$x_{(AB)}^{B}$	$x_{(AB)}^{'A}$	$x_{(AB)}^{'B}$
LiH	0.96	−0.96	0.08	0.02	0.97	0.02	0.98
LiF	0.97	−0.97	0.05	0.01	0.98	0.01	0.99
NaCl	0.98	−0.98	0.03	0.01	0.99	0.01	0.99
HF	0.70	−0.70	0.48	0.12	0.87	0.14	0.86
CO	0.57	−0.57	2.15	0.24	0.75	0.24	0.76
HCl	0.34	−0.34	0.91	0.33	0.67	0.34	0.66

TABLE VI. Covalent bond orders obtained in the orthogonal projector framework ($B_{AB}^{(SPA)}$) for the diatomic molecules in the test set. Values are calculated at the full-valence CASSCF/aug-cc-pVDZ level of theory.

	$B_{AB}^{(SPA)}$		$B_{AB}^{(SPA)}$
H_2	0.95	LiH	0.13
F_2	0.77	LiF	0.08
Cl_2	0.93	NaCl	0.05
Li_2	0.79	HF	0.54
O_2	1.35	CO	2.15
N_2	2.78	HCl	0.87
S_2	1.44		
P_2	2.64		

At the post-Hartree-Fock level, the number of electron pairs shared between the 1DMs $\rho_A{}^{(\infty)}$of the bonded atoms is generally lower than in Hartree-Fock (see Table VI). This can be roughly understood by considering that previously unoccupied orbitals in these atoms now have a small occupation, but contribute less efficiently to the bond order index than the previously fully occupied orbitals (with, e.g., σ and π shapes), whose occupation is now somewhat reduced. For the polar bonds, it is observed that some covalent bond order indices are larger with respect to the Hartree-Fock case. This is related to the less polar character of the bonds in these compounds at the correlated level (smaller atomic charges).

Calculations at the post-Hartree-Fock level are required to obtain reasonable indices for the covalent bond orders of molecules undergoing bond breaking and formation. As illustrated in Fig. 6 for N_2 and HF, Eq. (20) has the correct dissociation behavior at the full-valence CASSCF level, whereas the bond order index incorrectly evolves towards a constant nonzero value in the Hartree-Fock dissociation limit. Fig. 6(b) displays the covalent bond order of the polar HF molecule for bond lengths R_{AB} varying from the equilibrium bond length R_0. Fig. 6(c) displays the associated charge on the H-atom. Values for very short internuclear distances are

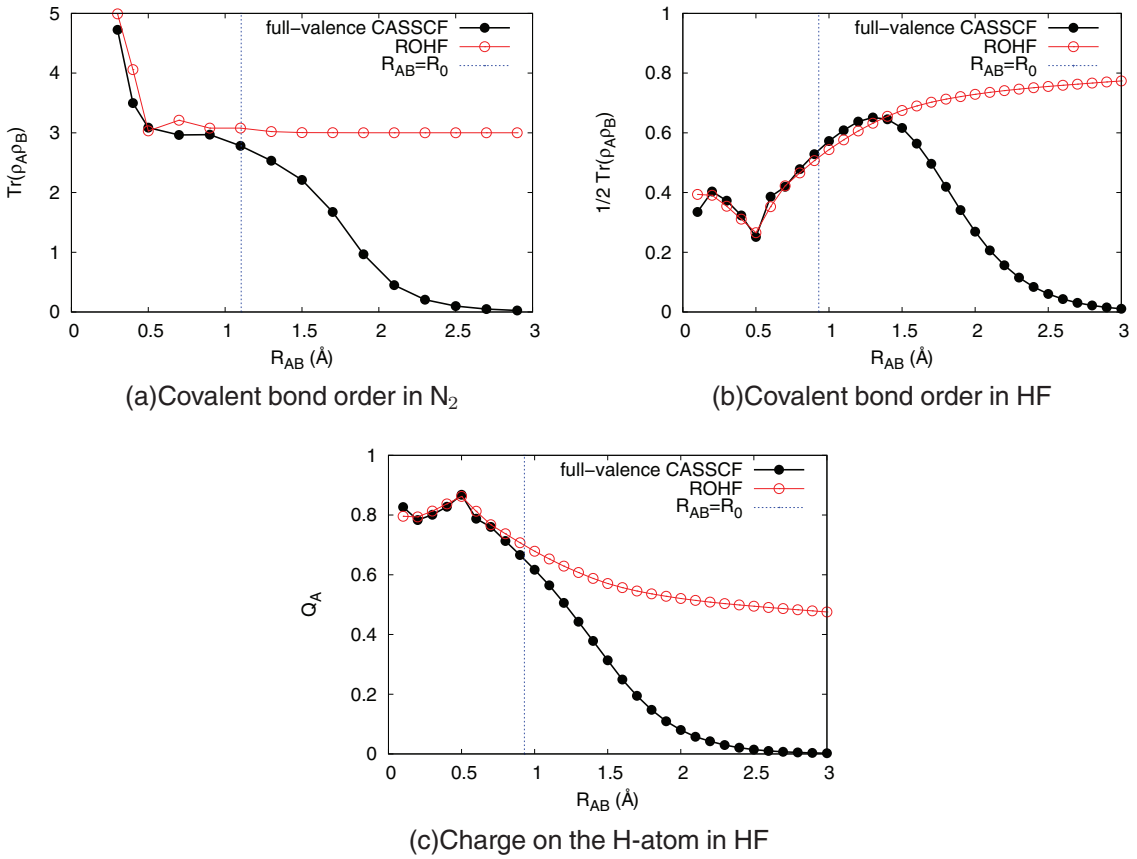

FIG. 6. Covalent bond order indices $B_{AB}^{(SPA)}$ in the N_2 and HF molecules for bond lengths R_{AB} varying from the equilibrium (B3LYP/aug-cc-pVDZ) bond length R_0. The covalent bond order index was determined at the RHF/aug-cc-pVDZ and full-valence CASSCF/aug-cc-pVDZ levels of theory.

chemically not relevant. It appears that covalent bond orders initially rise when the molecule starts dissociating, because atomic charges decrease and the molecule becomes less polar. At the dissociation limit, the CASSCF bond order and the atomic charges correctly drop to zero. The RHF bond order and atomic charges remain nonzero for large internuclear distances, and we checked that a value close to 1.0 is obtained at the dissociation limit. This is a typical RHF error. In UHF calculations, values for the covalent bond order fall to zero for large internuclear distances.

VII. CONCLUSIONS

Recently, we developed a double-atom partitioning of the molecular 1DM to describe atoms and bonds. The concept of atomic weight functions (familiar from Hirshfeld analysis of the electron density) is extended to atomic weight matrices. These weight matrices are determined iteratively by a stockholder approach, starting from the 1DMs of isolated atoms. The iterative procedure ensures that the weight matrices are orthogonal projectors on atomic subspaces, which has significant advantages in the interpretation of the bond contributions. This new scheme is referred to as SPA. All calculations are done in Hilbert space.

In the current paper, we provide evidence that chemically relevant orthogonal projection operators can be constructed using a recursive scheme. Numerical evidence was supplied for the recursive scheme used in Ref. 15 and solid theoretical proof could be obtained for a slightly adapted scheme.

We also examined the advantages associated with the SPA framework, with respect to transferability, bond orders and bond polarization. The atomic fragments of the molecular 1DM are clearly local. The final shape of the atomic orbitals is based on the isolated-atom 1DMs used as a starting point of the iterative procedure, but also reflects the molecular environment in a sense that these resemble fragmented bonding orbitals and free electron pairs. The populations of the orbitals associated with functional groups are remarkably constant. For the bond fragments, the analysis was focussed on covalent bond orders. The Hartree-Fock (HF) level of theory was applied to test the ability of the scheme to reproduce well-established information and known trends. In contrast to HF bond orders from a Hirshfeld-I analysis, HF covalent bond orders from the current scheme are small for ionic compounds and integer values are reproduced for homonuclear diatomic molecules. At the full-valence CASSCF level, covalent bond orders approximate typical Hartree-Fock values for equilibrium bond lengths, but (correctly) fall to zero at the dissociation limit. In the framework of orthogonal projectors, it is possible to assess approximately the contributions from the individual atoms to the covalent bond (order). These contributions provide a measure for the "dative" character of covalent bonds.

ACKNOWLEDGMENTS

D.V.F., D.V.N., P.B., and D.G. acknowledge support from the research council (BOF) of Ghent University and FWO-Vlaanderen. P.W.A. acknowledges support from Sharcnet, NSERC, and the Canada Research Chairs.

APPENDIX: ANALYTICAL PROOFS OF SEC. II

Lemma 2.1. *If $M = \rho^{(i-1)}$ in Eq. (7), then the converged weight matrices $w_A^{(\infty)}$ are idempotent.*

Proof: If $M = \rho^{(i-1)}$ in Eq. (7), then we can use the shorthand notation,

$$w_A^{(\infty)} \rho^{(\infty)} w_A^{(\infty)} = \rho_{AA}^{'(\infty)}, \tag{A1}$$

to write down the converged solution of the recursive scheme in Eq. (7):

$$w_A^{(\infty)} = (\rho^{(\infty)})^{-\frac{1}{2}} \rho_{AA}^{'(\infty)} (\rho^{(\infty)})^{-\frac{1}{2}} \tag{A2}$$

$$\rho^{(\infty)} = \sum_A \rho_{AA}^{'(\infty)}. \tag{A3}$$

By substituting Eq. (A2) in Eq. (A1), we obtain an equation,

$$(\rho^{(\infty)})^{-\frac{1}{2}} \rho_{AA}^{'(\infty)} \rho_{AA}^{'(\infty)} (\rho^{(\infty)})^{-\frac{1}{2}} = \rho_{AA}^{'(\infty)}, \tag{A4}$$

that can be multiplied on both sides by $\rho_{AA}^{'(\infty)}$ so that the square root of the resulting expression becomes

$$\rho_{AA}^{'(\infty)} (\rho^{(\infty)})^{-\frac{1}{2}} \rho_{AA}^{'(\infty)} = (\rho_{AA}^{'(\infty)})^{\frac{3}{2}}. \tag{A5}$$

After multiplying the left side of Eq. (A4) by $\rho_{AA}^{'(\infty)} (\rho^{(\infty)})^{-\frac{1}{2}}$ and the right side by $(\rho^{(\infty)})^{-\frac{1}{2}} \rho_{AA}^{'(\infty)}$, the square root of that expression can be simplified on the right hand side by twice substituting Eq. (A5) into it,

$$\begin{aligned} \rho_{AA}^{'(\infty)} (\rho^{(\infty)})^{-1} \rho_{AA}^{'(\infty)} &= \left(\rho_{AA}^{'(\infty)} (\rho^{(\infty)})^{-\frac{1}{2}} \rho_{AA}^{'(\infty)} (\rho^{(\infty)})^{-\frac{1}{2}} \rho_{AA}^{'(\infty)}\right)^{\frac{1}{2}} \\ &= \left((\rho_{AA}^{'(\infty)})^{\frac{3}{2}} (\rho^{(\infty)})^{-\frac{1}{2}} \rho_{AA}^{'(\infty)}\right)^{\frac{1}{2}} \\ &= \left(\left(\rho_{AA}^{'(\infty)}\right)^{\frac{1}{2}} \left(\rho_{AA}^{'(\infty)}\right)^{\frac{3}{2}}\right)^{\frac{1}{2}} \\ &= \rho_{AA}^{'(\infty)}. \end{aligned} \tag{A6}$$

A simple multiplication of Eq. (A6) on both sides with $(\rho^{(\infty)})^{-\frac{1}{2}}$ retrieves

$$\left(w_A^{(\infty)}\right)^2 = w_A^{(\infty)}, \tag{A7}$$

establishing that the atomic weight matrices are idempotent or binary in Hilbert space.

Lemma 2.2. *If the converged weight matrices $w_A^{(\infty)}$ are idempotent, then they are orthogonal.*

Proof: Suppose that $x_{B,j}$ is a normalized eigenvector of $w_B^{(\infty)}$ with unit eigenvalue. Then

$$x_{B,j}^T \left(\sum_A w_A^{(\infty)}\right) x_{B,j} = x_{B,j}^T I x_{B,j} = x_{B,j}^T x_{B,j} = 1. \tag{A8}$$

The left hand side of Eq. (A8) can be rewritten,

$$x_{B,j}^T\left(w_B^{(\infty)}\right)x_{B,j} + x_{B,j}^T\left(\sum_{A\neq B} w_A^{(\infty)}\right)x_{B,j} = 1$$

$$1 + x_{B,j}^T\left(\sum_{A\neq B} w_A^{(\infty)}\right)x_{B,j} = 1, \quad \text{(A9)}$$

and therefore we have

$$\sum_{A\neq B} x_{B,j}^T\left(w_A^{(\infty)}\right)x_{B,j} = 0. \quad \text{(A10)}$$

However, since the atomic weight matrices are positive semidefinite by construction, this implies that for every A ≠ B:

$$x_{B,j}^T\left(w_A^{(\infty)}\right)x_{B,j} = 0,$$

$$\left(w_A^{(\infty)}\right)x_{B,j} = \mathbf{0}. \quad \text{(A11)}$$

And so any eigenvector of $w_B^{(\infty)}$ with unit eigenvalue is an eigenvector of all the other weight matrices with zero eigenvalue. An explicit way to show that binary weight matrices are orthogonal is to expand an arbitrary trial vector in the eigenbasis of $w_B^{(\infty)}$. Then

$$w_A^{(\infty)}w_B^{(\infty)}\left(\sum_j c_j x_{B,j}\right) = \mathbf{0}, \quad \text{(A12)}$$

because either $(w_B^{(\infty)}x_{B,j} = \mathbf{0})$ or $(w_B^{(\infty)}x_{B,j} = x_{B,j}$ and $w_A^{(\infty)}x_{B,j} = \mathbf{0})$.

Since Eq. (A12) is true for every trial vector, this implies that the weight matrices must be orthogonal:

$$w_A^{(\infty)}w_B^{(\infty)} = \mathbf{0}. \quad \text{(A13)}$$

Lemma 2.3. *When idempotent weight matrices enter the recursive scheme of Eq. (7), immediate convergence is obtained.*

Proof: With the shorthand notation,

$$\rho_{AA}^{'(i)} = w_A^{(i-1)}Mw_A^{(i-1)}, \quad \text{(A14)}$$

and the assumption that for iteration (*i*-1) the weight matrices are binary $[w_A^{(i-1)} = (w_A^{(i-1)})^2]$, the following equation is obtained:

$$\rho_{AA}^{'(i)} = w_A^{(i-1)}\rho_{AA}^{'(i)}w_A^{(i-1)}. \quad \text{(A15)}$$

When both sides of this equation are multiplied by $(\rho_{AA}^{'(i)})^{\frac{1}{2}}$, and the square root of the resulting expression is multiplied once more on both sides by $(\rho_{AA}^{'(i)})^{\frac{1}{2}}$, we arrive at

$$\left(\rho_{AA}^{'(i)}\right)^2 = \rho_{AA}^{'(i)}w_A^{(i-1)}\rho_{AA}^{'(i)}. \quad \text{(A16)}$$

Since the weight matrices are binary and therefore orthogonal, if follows from $\rho^{(i)} = \sum_A \rho_{AA}^{'(i)}$ that

$$\left(\rho_{AA}^{'(i)}\right)^2 = \rho^{(i)}w_A^{(i-1)}\rho^{(i)}, \quad \text{(A17)}$$

and the result can be rewritten in terms of the weight matrices for iteration (*i*-1) and (*i*):

$$w_A^{(i-1)} = (\rho^{(i)})^{-1}\left(\rho_{AA}^{'(i)}\right)^2(\rho^{(i)})^{-1},$$

$$w_A^{(i-1)} = (\rho^{(i)})^{-\frac{1}{2}}\left((\rho^{(i)})^{-\frac{1}{2}}\rho_{AA}^{'(i)}(\rho^{(i)})^{-\frac{1}{2}}\right)$$

$$\times\rho^{(i)}\left((\rho^{(i)})^{-\frac{1}{2}}\rho_{AA}^{'(i)}(\rho^{(i)})^{-\frac{1}{2}}\right)(\rho^{(i)})^{-\frac{1}{2}},$$

$$w_A^{(i-1)} = (\rho^{(i)})^{-\frac{1}{2}}w_A^{(i)}\rho^{(i)}w_A^{(i)}(\rho^{(i)})^{-\frac{1}{2}}. \quad \text{(A18)}$$

A similar relationship between the weight matrices for iteration (*i*-1) and (*i*) can be obtained, starting from the definitions of $w_A^{(i)}$ and $\rho_{AA}^{'(i)}$:

$$w_A^{(i)} = (\rho^{(i)})^{-\frac{1}{2}}\rho_{AA}^{'(i)}(\rho^{(i)})^{-\frac{1}{2}},$$

$$w_A^{(i)} = (\rho^{(i)})^{-\frac{1}{2}}w_A^{(i-1)}Mw_A^{(i-1)}(\rho^{(i)})^{-\frac{1}{2}}. \quad \text{(A19)}$$

Matrix *M* can be substituted, using the idempotency and orthogonality for the weight functions,

$$w_A^{(i-1)}Mw_A^{(i-1)} = \left(w_A^{(i-1)}\right)^2M\left(w_A^{(i-1)}\right)^2$$

$$= \left(w_A^{(i-1)}\right)\rho_{AA}^{'(i)}\left(w_A^{(i-1)}\right)$$

$$= \left(w_A^{(i-1)}\right)\rho^{(i)}\left(w_A^{(i-1)}\right), \quad \text{(A20)}$$

after which the relationship between the weight matrices for iteration (*i*-1) and (*i*) (Eq. (A19)) becomes

$$w_A^{(i)} = (\rho^{(i)})^{-\frac{1}{2}}w_A^{(i-1)}\rho^{(i)}w_A^{(i-1)}(\rho^{(i)})^{-\frac{1}{2}}. \quad \text{(A21)}$$

Equations (A18) and (A21) are equal apart from interchanging $w_A^{(i-1)}$ and $w_A^{(i)}$. Therefore, when the system of these equations is solved with the substitution method, it appears that

$$w_A^{(i-1)} = w_A^{(i)}. \quad \text{(A22)}$$

Lemma 2.4. *If $M = \rho$ in the recursive scheme of Eq. (7), then it is in principle not excluded that particular non-idempotent solutions $w_A^{(\infty)}$ result from the recursion.*

Proof: The convergence limit of the iterative scheme is

$$w_A^{(\infty)} = (\rho^{(\infty)})^{-\frac{1}{2}}w_A^{(\infty)}Mw_A^{(\infty)}(\rho^{(\infty)})^{-\frac{1}{2}},$$

$$\rho^{(\infty)} = \sum_A w_A^{(\infty)}Mw_A^{(\infty)}. \quad \text{(A23)}$$

We have, then, that

$$(\rho^{(\infty)})^{\frac{1}{2}}w_A^{(\infty)}(\rho^{(\infty)})^{\frac{1}{2}} = w_A^{(\infty)}Mw_A^{(\infty)}. \quad \text{(A24)}$$

Consider a system with k fragments. Suppose that all the fragments had the same weight matrix,

$$w_A^{(\infty)} = \frac{1}{k}I. \quad \text{(A25)}$$

Then

$$\rho^{(\infty)} = \sum_A\left(\frac{1}{k}I\right)M\left(\frac{1}{k}I\right) = \frac{1}{k}M. \quad \text{(A26)}$$

Inserting into Eq. (A24) reveals that this is also a particular solution,

$$(\rho^{(\infty)})^{\frac{1}{2}}w_A^{(\infty)}(\rho^{(\infty)})^{\frac{1}{2}} = w_A^{(\infty)}Mw_A^{(\infty)}$$

$$\left(\frac{1}{k}M\right)^{\frac{1}{2}}\left(\frac{1}{k}I\right)\left(\frac{1}{k}M\right)^{\frac{1}{2}} = \left(\frac{1}{k}I\right)M\left(\frac{1}{k}I\right)$$

$$\frac{1}{k^2}M = \frac{1}{k^2}M. \quad \text{(A27)}$$

[1]R. S. Mulliken, J. Chem. Phys. **23**, 1833 (1955).
[2]R. F. W. Bader, Chem. Rev. **91**, 893 (1991).
[3]R. F. W. Bader, *Atoms in Molecules: A Quantum Theory*, The International Series of Mono-graphs on Chemistry Vol. 22 (Oxford University Press, Oxford, 1994).
[4]P. Popelier, *Atoms In Molecules: An Introduction* (Prentice-Hall, Harlow, England, 2000).
[5]F. L. Hirshfeld, Theor. Chim. Acta **44**, 129 (1977).
[6]P. Bultinck, C. Van Alsenoy, P. W. Ayers, and R. Carbó-Dorca, J. Chem. Phys. **126**, 144111 (2007).
[7]P. Bultinck, Faraday Discuss. **135**, 244 (2007).
[8]P. Bultinck, P. W. Ayers, S. Fias, K. Tiels, and C. Van Alsenoy, Chem. Phys. Lett. **444**, 205 (2007).
[9]P. Bultinck, D. L. Cooper, and D. Van Neck, Phys. Chem. Chem. Phys. **11**, 3424 (2009).
[10]T. C. Lillestolen and R. J. Wheatley, Chem. Commun. **45**, 5909 (2008).
[11]L. Li and R. G. Parr, J. Chem. Phys. **84**, 1704 (1986).
[12]D. Vanfleteren, D. Van Neck, P. Bultinck, P. W. Ayers, and M. Waroquier, J. Chem. Phys. **132**, 164111 (2010).
[13]D. Vanfleteren, D. Ghillemijn, D. Van Neck, P. Bultinck, M. Waroquier, and P. W. Ayers, J. Comput. Chem. **32**(16), 3485 (2011).
[14]I. Mayer and P. Salvador, J. Chem. Phys. **130**, 234106 (2009).
[15]D. Vanfleteren, D. Van Neck, P. Bultinck, P. W. Ayers, and M. Waroquier, J. Chem. Phys. **133**, 231103 (2010).
[16]P. O. Lowdin, J. Chem. Phys. **18**, 365 (1950).
[17]P. O. Lowdin, Adv. Quantum Chem. **5**, 185 (1970).
[18]E. R. Davidson, J. Chem. Phys. **46**, 3320 (1967).
[19]K. R. Roby, Mol. Phys. **27**, 81 (1974).
[20]M. S. Gopinathan and K. Jug, Theor. Chim. Acta **63**, 497 (1983).
[21]A. E. Reed, R. B. Weinstock and F. Weinhold J. Chem. Phys. **83**, 735 (1985).
[22]K. Kullback and R. A. Leibler, Ann. Math. Stat. **22**, 79 (1951).
[23]R. F. Nalewajski and R. G. Parr, Proc. Natl. Acad. Sci. U.S.A. **97**, 8879 (2000).
[24]R. F. Nalewajski and R. G. Parr, J. Phys. Chem. A **105**, 7391 (2001).
[25]W. T. Yang, Y. K. Zhang, and P. W. Ayers, Phys. Rev. Lett. **84**, 5172 (2000).
[26]Y. K. Zhang and W. T. Yang, Theor. Chem. Acc. **103**, 346 (2000).
[27]P. W. Ayers, J. Math. Chem. **43**, 285 (2008).
[28]K. B. Wiberg, Tetrahedron **24**, 1083 (1968).
[29]R. F. W. Bader and M. E. Stephens, J. Am. Chem. Soc. **97**, 7391 (1975).
[30]M. Giambiagi, M. S. de Giambiagi, D. R. Grempel, and C. D. Heymann, J. Chim. Phys. **72**, 15 (1975).
[31]I. Mayer, Chem. Phys. Lett. **97**, 270 (1983).
[32]R. L. Fulton, J. Phys. Chem. **97**, 7516 (1993).
[33]J. G. Angyan, M. Loos, and I. Mayer, J. Phys. Chem. **98**, 5244 (1994).
[34]X. Fradera, M. A. Austen, and R. F. W. Bader, J. Phys. Chem. A **103**, 304 (1999).
[35]I. Mayer and P. Salvador, Chem. Phys. Lett. **383**, 368 (2004).
[36]R. Ponec and D. L. Cooper, J. Mol. Struct. (Theochem) **727**, 133 (2005).
[37]I. Mayer, J. Comput. Chem. **28**, 204 (2007).
[38]A. D. Becke, J. Chem. Phys. **98**, 5648 (1993).
[39]C. Lee, W. Yang, and R. G. Parr, Phys. Rev. B **37**, 785 (1988).
[40]S. H. Vosko, L. Wilk, and M. Nusair, Can. J. Phys. **58**, 1200 (1980).
[41]P. J. Stephens, F. J. Devlin, C. F. Chabalowski, and M. J. Frisch, J. Phys. Chem. **98**, 11623 (1994).
[42]D. E. Woon and T. H. Dunning, J. Chem. Phys. **98**, 1358 (1993).
[43]B. P. Prascher, D. E. Woon, K. A. Peterson, T. H. Dunning, Jr., and A. K. Wilson, Theor. Chem. Acc. **128**, 69 (2011)
[44]T. H. Dunning, J. Chem. Phys. **90**, 1007 (1989).
[45]R. A. Kendall, T. H. Dunning, and R. J. Harrison, J. Chem. Phys. **96**, 6796 (1992).